JOURNAL OF MATERIALS SCIENCE **33** (1998) 5821–5825

# A kinetic study of the thermal decomposition of ammoniojarosite

M. ALONSO, A. LÓPEZ-DELGADO, F. A. LÓPEZ*
*Department of Materials Recycling, National Centre for Metallurgical Research (CSIC), Avda. Gregorio del Amo, 8, E-28040 Madrid, Spain*
*E-mail: flopez@fresno.csic.es*

Polycrystalline powdered ammoniojarosite was obtained by hydrolysis from bio-oxidized sulphuric pickling waste water. The kinetic parameters of the thermal decomposition process of ammoniojarosite were calculated by means of thermogravimetric measurements. Analyses were performed in non-isothermal conditions at different heating rates. The three stages of the thermal decomposition process (dehydration, dehydroxylation and deammoniation, and sulphate decomposition) are best described by the Avrami–Erofeev $A_m$ model. The kinetic exponent $m$ increases, in general, with the heating rate. Apparent activation energies of 54, 244 and 130 kJ mol$^{-1}$, respectively, were obtained for each decomposition stage. 

## 1. Introduction

Ammoniojarosite, $NH_4Fe_3(SO_4)_2(OH)_6$, is a commonly known mineral of the jarosite family. The precipitation of iron in the form of a jarosite compound is a low-cost technology widely employed in the industry, especially in the zinc industry, in order to remove iron and other metallic impurities [1]. Iron (III) oxide by-products are obtained by means of a further thermal treatment of jarosites [2, 3]. Depending on the physico-chemical properties, iron oxides are used in pigments, magnetic materials and clinker productions. The properties of the decomposition product are affected, among others, by the kinetics of the thermal decomposition process. Therefore, a decomposition kinetic study is a necessary prerequisite if control of the decomposition product properties is required. Thus, in this work, a kinetic study of the thermal decomposition of ammoniojarosite was attempted. Analyses were performed in non-isothermal conditions. Reaction rate parameters corresponding to the different stages of the decomposition process were calculated and the rate-controlling process for each one has been proposed.

## 2. Experimental procedure

Ammoniojarosite was prepared by hydrolysis from a bio-oxidized sulphuric pickling water (BSPW). Sulphuric pickling water is a waste product from the steelmaking industry. A detailed description of the bio-oxidation procedure has been published elsewhere [4, 5]. The chemical composition (g l$^{-1}$) of the bio-oxidized sulphuric pickling solution employed in this work, is $Fe^{3+} = 8.6$, $NH_4^+ = 7.7$ and $(SO_4^{2-})_{total} = 40.92$. The pH value of solution is 1.54 and the free sulphuric acid content is 0.03 M.

BSPW hydrolysis was carried out in a sealed vessel at 160 °C for 2 h. After cooling, the vessel was opened and the solids and mother liquors were separated and analysed. The solids obtained were washed with water until negative sulphate reaction, and dried at 100 °C for 24 h. The complete characterization of ammoniojarosite has been previously reported [6].

Thermogravimetric (TG) measurements were done employing a Shimadzu TGA-50H instrument. Non-isothermal TG curves were recorded up to 800 °C at heating rates of 10, 11, 13, 15, 17 and 20 °C min$^{-1}$. Samples of 10 mg were used in each test. All the decomposition experiments were performed in alumina crucibles (diameter = 5 mm, $h = 3$ mm) in a flowing nitrogen atmosphere (20 ml min$^{-1}$).

## 3. Results and discussion

TGA curves recorded on ammoniojarosite at different heating rates are depicted in Fig. 1. The decomposition process occurs in three steps. The first takes place between 60 and 330 °C with a weigh loss of approximately 2%, and can be attributed to dehydration of coordinated water

$$NH_4Fe_3(SO_4)_2(OH)_6 \cdot H_2O \rightarrow NH_4Fe_3(SO_4)_2(OH)_6 + H_2O \quad (1)$$

Frequently, jarosites are described with coordination water molecules, their presence being explained by non-bridged sites in the octahedral coordination polyhedron of the ferric ions [7].

The second weight loss occurring up to 480 °C is due to both the dehydroxylation and deammoniation of ammoniojarosite according to the equation

* Author to whom all correspondence should be addressed.

TABLE I TGA results for different heating rates

| Heating rate (°C min$^{-1}$) | Step 1 | | Step 2 | | Step 3 | |
|---|---|---|---|---|---|---|
| | $T_p$[a] (°C) | Weight loss (%) | $T_p$[a] (°C) | Weight loss (%) | $T_p$[a] (°C) | Weight loss (%) |
| 10 | 291 | 1.95 | 427 | 12.34 | 668 | 28.50 |
| 11 | 286 | 2.11 | 423 | 13.66 | 667 | 29.55 |
| 13 | 298 | 2.26 | 427 | 14.06 | 665 | 29.78 |
| 15 | 293 | 1.79 | 433 | 14.26 | 675 | 30.47 |
| 17 | 300 | 1.40 | 432 | 14.49 | 681 | 31.13 |
| 20 | 300 | 2.05 | 434 | 13.39 | 690 | 29.76 |

[a] Peak temperature in the differential TGA plot.

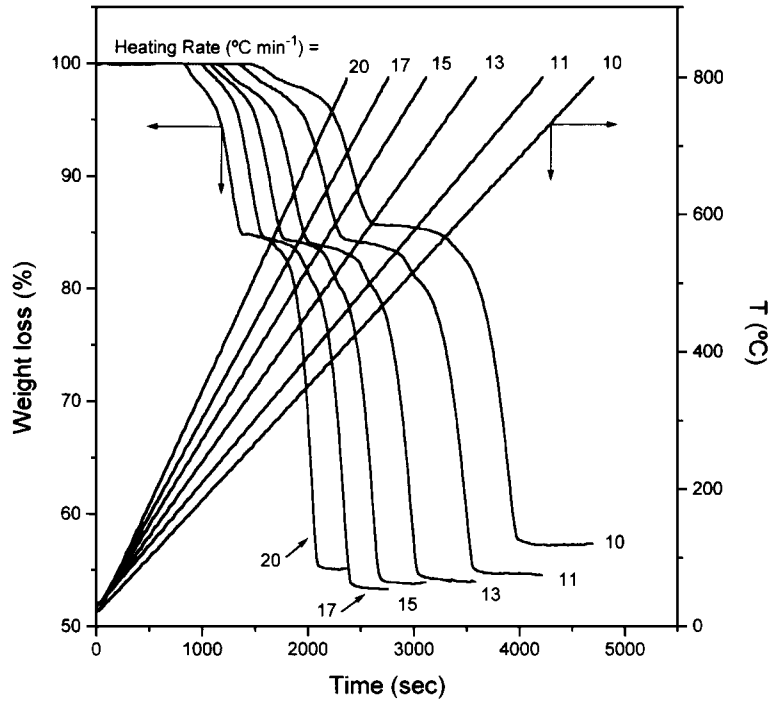


*Figure 1* Thermogravimetric curves for different heating rates.

$$NH_4Fe_3(SO_4)_2(OH)_6 \rightarrow 2/3\ Fe_2(SO_4)_3 + 5/6\ Fe_2O_3 + NH_3 + 7/2\ H_2O \quad (2)$$

The losses of water and ammonia take place in the same stage [6, 8, 9].

The third and last step corresponds to thermal decomposition of Fe(III) sulphate formed in the previous stage. The loss of $SO_3$ content leads to the formation of $\alpha Fe_2O_3$ as the final product

$$Fe_2(SO_4)_3 \rightarrow \alpha Fe_2O_3 + 3\ SO_3(g) \quad (3)$$

The weight losses and the temperatures corresponding to each decomposition stage at different heating rates are presented in Table I. Generally, the faster the heating rate, the higher the peak temperature. The variation of weight loss with heating rate is irregular.

In order to study the mechanism of the thermal decomposition of ammoniojarosite, both the activation energy and the rate-controlling reaction were determined. The general kinetic equation can be written as

$$\frac{dx}{dt} = kf(x) \quad (4)$$

where $x$ is the reacted mass fraction of a given reactant, which can be straightforwardly calculated from the weight loss data provided by the TG experiments, $t$ is the time, $k$ the rate constant and $f(x)$ a certain function of the reacted mass fraction [10–12]. Assuming that the Arrhenius law can be applied to the solid-state reactions, the rate constant can be expressed as

$$k = Ae^{-E/RT} \quad (5)$$

where $A$ is the frequency or pre-exponential factor, $E$ the activation energy, $R$ the gas constant and $T$ the absolute temperature. Equation 4 can be written for various heating rates as

$$\frac{dx}{f(x)} = \frac{1}{\phi} Ae^{-E/RT}\, dT \quad (6)$$

where $\phi = dT/dt$ is the heating rate. A given value of the conversion, $x$, is attained at a value of the temperature which depends on the particular heating rate at which the reaction is taking place. The TG curves obtained at different heating rates, $\phi$, enable us to form sets of points having the same value of $x$ and different temperatures. For any of these sets, the left-hand side of

TABLE II Kinetic model functions $f(x)$ applied for the solid-state reactions of thermal decomposition of ammoniojarosite

| Function, $f(x)$ | Symbol | Rate-controlling process |
|---|---|---|
| $\frac{1}{2x}$ | $D_1$ | One-dimensional diffusion |
| $-\frac{1}{\ln(1-x)}$ | $D_2$ | Two-dimensional diffusion, cylindrical symmetry |
| $\frac{3(1-x)^{2/3}}{2[1-(1-x)^{2/3}]}$ | $D_3$ | Three-dimensional diffusion, spherical symmetry; Jander equation |
| $\frac{3}{2[(1-x)^{-1/3}-1]}$ | $D_4$ | Three-dimensional diffusion, spherical symmetry; Ginstring-Brounshtein |
| $n(1-x)^{1-1/n}$ | $R_n(1 \leq n \leq 3)$ | Phase boundary reaction |
| $m(1-x)[-\ln(1-x)]^{1-1/m}$ | $A_m(0.5 \leq m \leq 4)$ | Nucleation and growth; Avrami–Erofeev equation |

TABLE III Kinetic parameters obtained for the non-isothermal decomposition of ammoniojarosite

| Heating rate | Dehydratation (250–330 °C) $E = 54$ kJ mol$^{-1}$ | | | Dehydroxylation/deammoniation (330–480 °C) $E = 244$ kJ mol$^{-1}$ | | | Decomposition of ferric sulphate (500–720 °C) $E = 130$ kJ mol$^{-1}$ | | |
|---|---|---|---|---|---|---|---|---|---|
| (°C min$^{-1}$) | Model | $A$ (l s$^{-1}$) | $\gamma$[a] | Model | $A$ (l s$^{-1}$) | $\gamma$[a] | Model | $A$ (l s$^{-1}$) | $\gamma$[a] |
| 10 | $A_m(m = 1.5)$ | 468 | 0.9985 | $A_m(m = 0.6)$ | $3.99 \times 10^{16}$ | 0.9828 | $A_m(m = 1.9)$ | $7.15 \times 10^4$ | 0.9946 |
| 11 | $A_m(m = 1.6)$ | 450 | 0.9990 | $A_m(m = 0.5)$ | $3.89 \times 10^{16}$ | 0.9888 | $A_m(m = 1.7)$ | $8.4 \times 10^4$ | 0.9919 |
| 13 | $A_m(m = 1.5)$ | 539 | 0.9995 | $A_m(m = 0.6)$ | $2.74 \times 10^{16}$ | 0.9917 | $A_m(m = 1.8)$ | $10.0 \times 10^4$ | 0.9948 |
| 15 | $A_m(m = 1.6)$ | 593 | 0.9988 | $A_m(m = 0.6)$ | $2.56 \times 10^{16}$ | 0.9963 | $A_m(m = 1.9)$ | $9.5 \times 10^4$ | 0.9949 |
| 17 | $A_m(m = 1.9)$ | 659 | 0.9991 | $A_m(m = 0.7)$ | $2.21 \times 10^{16}$ | 0.9976 | $A_m(m = 2.0)$ | $9.5 \times 10^4$ | 0.9939 |
| 20 | $A_m(m = 1.9)$ | 774 | 0.9989 | $A_m(m = 0.9)$ | $1.74 \times 10^{16}$ | 0.9947 | $A_m(m = 2.2)$ | $9.2 \times 10^4$ | 0.9938 |

[a] Correlation coefficient.

Equation 6 is a constant, and so must be the right-hand side. Therefore, plotting $\ln \phi$ against $1/T$ for any set of points with $x = \text{const}$, should yield a straight line

$$\ln \phi = \text{constant} - \frac{E}{RT} \tag{7}$$

from whose slope the activation energy, $E$, can be evaluated.

The three reactions involved in the thermal decomposition, namely dehydration (Reaction 1), dehydroxylation and deammoniation (Reaction 2), and sulphate decomposition (Reaction 3), were analysed independently. The variation of the logarithm of the heating rate with reciprocal temperature for constant values of $x$, corresponding to each step of thermal decomposition is given in Fig. 2. From the slope of these curves, the activation energy was calculated.

For the dehydration process, step 1, the activation energy obtained for each value of $x$, Fig. 2a, fluctuates with no systematic tendency between 38.7 and 57.7 kJ mol$^{-1}$. The average value, 53.9 kJ mol$^{-1}$ was taken as the activation energy, $E$, for this process.

For the second and third stages of the decomposition process, 244.1 kJ mol$^{-1}$ and 130.6 kJ mol$^{-1}$ were the average activation energy (Fig. 2b and 2c), respectively.

Integration of Equation 4 gives

$$\int_0^x \frac{\mathrm{d}x}{f(x)} = A \int_{t_0}^t e^{-E/RT} \mathrm{d}t \tag{8}$$

where $t_0$ is the time at which $x = 0$. Once the activation energy, and hence the integral of the right-hand side of Equation 8, is known, regression analyses are performed using different kinetic model functions $f(x)$. The rate-controlling mechanism is then taken to be that yielding the highest correlation coefficient. Table II summarizes the functions tested for the solid-state reactions [10].

The dehydration process of ammoniojarosite, Equation 1, in non-isothermal conditions is best described by the Avrami–Erofeev $A_m$ model, although the contracting geometry $R_n$ model was not very inferior. The $m$ value ranged between 1.5 and 1.9 depending on the heating rate employed. Both the subindex $m$ and the pre-exponential factor $A$ increase with heating rate. As an example, the plot of the reacted mass fraction, $x$, against the temperature, $T$, for the dehydration process at the heating rate of 20 °C min$^{-1}$, is shown in Fig. 3a along with the theoretical curve obtained by applying the $A_m$ ($m = 1.9$) law.

The kinetic parameters obtained for each heating rate and for the three stages of thermal decomposition of ammoniojarosite are listed in Table III. The correlation coefficients are also included in this table.

The kinetics of the second reaction (Equation 2) also obeys to the $A_m$ model; $0.5 \leq m \leq 0.9$ is the value of the kinetic exponent $m$ obtained for the different heating rates. The faster the heating rate, the higher is the value of $m$. However, in this reaction, the pre-exponential factor value decreases with the heating rate. The experimental $x$ versus $T$ plot obtained from TG analysis at a heating rate of 20 °C min$^{-1}$ is well reproduced by the $A_m$ ($m = 0.9$) model as shown in Fig. 3b.

For the decomposition of ferric sulphate, Equation 3, the same kinetic model was found as for the former reaction. In this case, the highest values of the kinetic exponent $m$ were obtained, especially at a heating rate of 20 °C min$^{-1}$. The variation of $A$ is irregular, its higher value being obtained at a heating rate of 13 °C min$^{-1}$. The experimental and calculated variations of the reacted fraction with the temperature (at heating rate of 20 °C min$^{-1}$) are shown in Fig. 3c.

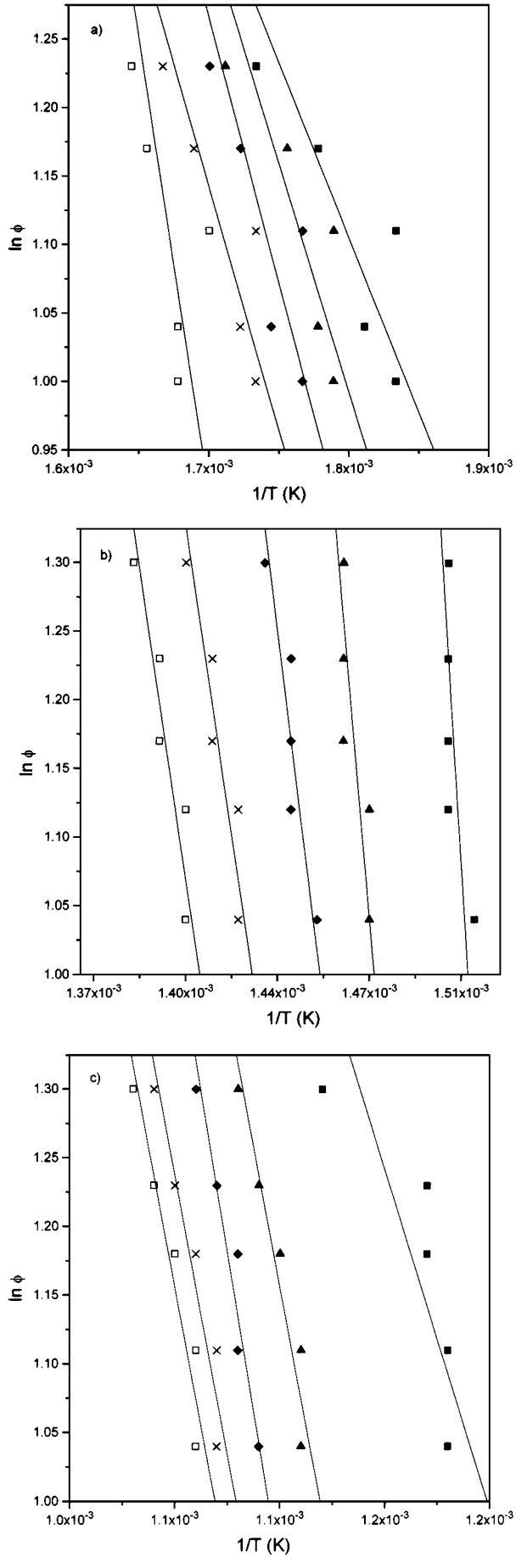


*Figure 2* Plots of $\ln\phi$ versus $1/T$ for the (a) dehydration, (b) dehydroxylation and deammoniation, and (c) ferric sulphate decomposition processes.

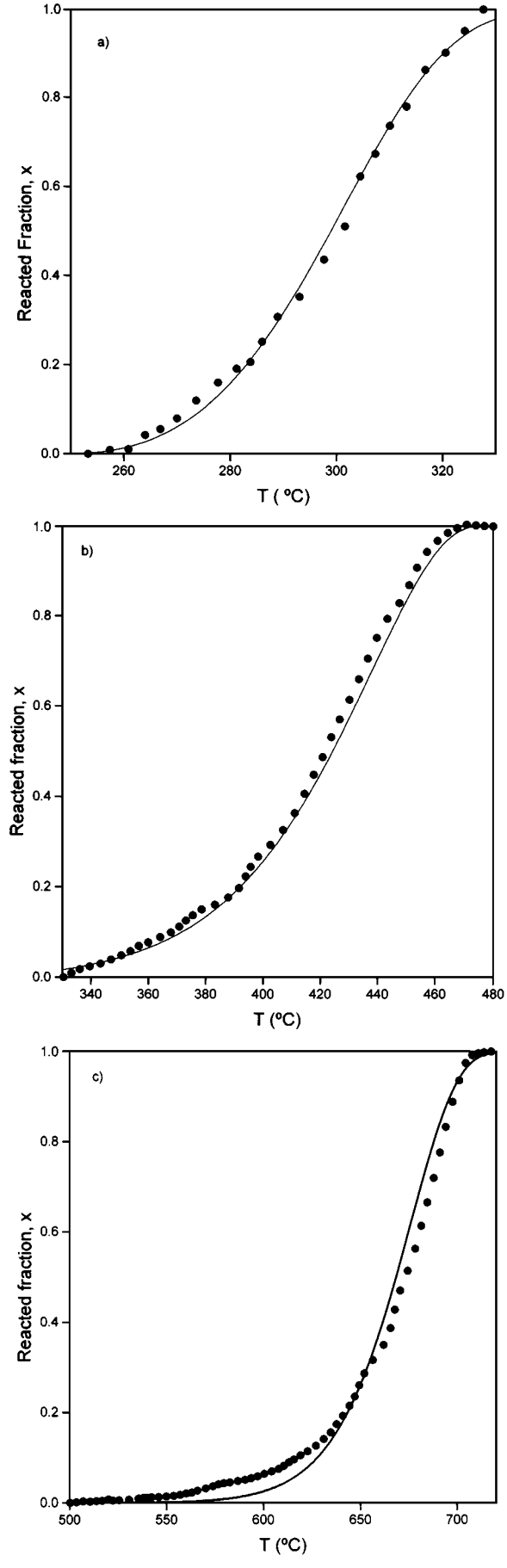


*Figure 3* Plots of reacted fraction, $x$, versus temperature, $T$ (°C) for the (a) dehydration, (b) dehydroxylation and deammoniation, and (c) ferric sulphate decomposition processes at a heating rate of 20 °C $\text{min}^{-1}$. (●) Experimental and (——) calculated data from the $A_m$ model.

The overall thermal decomposition of ammoniojarosite in non-isothermal conditions can be considered to be controlled by nucleation and growth type equations, according to our experimental results. The kinetic obedience of the Avrami–Erofeev law involves the previous existence of potential sites for nucleation, with the rate of advancement of the reaction interface being controlled by diffusion.

## References


1. M. PELINO, C. CANTALINI, C. ABBRUZZESE and P. PESCIA, *Hydrometall*. **40** (1996) 25.
2. J. E. DUTRIZAC, *J. Metals* **1** (1990) 36.
3. Z. SOLC, M. TROJAN, D. BRANDOVÁ and M. KUCHLER, *J. Thermal Anal*. **33** (1988) 463.
4. F. J. GARCÍA, A. RUBIO, E. SÁINZ, P. GONZÁLEZ and F. A. LÓPEZ, *FEMS Microb. Rev*. **14** (1994) 397.
5. F. A. LÓPEZ, A. LÓPEZ-DELGADO and F. J. GARCÍA, edited by O. Bitchaeva and C. Ronneau, in "Biotechnologies for Wastes Management and Site Restoration," Edited by Kluwer Academic Publisher. Dordrecht, The Netherlands, 1997.
6. A. LÓPEZ-DELGADO, F. J. ALGUACIL and F. A. LÓPEZ, *Hydrometall*. **45** (1997) 97.
7. N. LAZAROFF, W. SIGAL and A. WASSERMAN, *Appl. Environ. Microbiol*. **43** (1982) 924.
8. F. PAULIK and J. PAULIK, *J. Thermal Anal*. **5** (1973) 253.
9. G. K. DAS, S. ANAND, S. ACHARYA and R. P. DAS, *Hydrometall*. **38** (1995) 263.
10. J. H. SHARP, G. W. BRINDLEY and B. N. N. ACHAR, *J. Am. Ceram. Soc*. **49** (1966) 379.
11. H. TANAKA, *Thermochim. Acta* **267** (1995) 29.
12. D. DOLLIMORE, P. TONG and K. S. ALEXANDER, *ibid*. **282/283** (1996) 13.



*Received 9 September 1997*
*and accepted 23 July 1998*